

Electronic Supplementary Information for

High-Yield and environment-minded fabrication of nanoporous anodic aluminum oxide templates

Young Ki Hong,^{ab} Bo Hyun Kim,^a Dong Il Kim,^a Dong Hyun Park,^{ac} and Jinsoo Joo^{*a}

^aDepartment of Physics, Korea University, Seoul 136-713, South Korea.

^bDepartment of Electronics and Radio Engineering, Kyung Hee University, Gyeonggi 446-701, South Korea.

^cDepartment of Applied Organic Materials Engineering, Inha University, Incheon 402-751, South Korea.

*Address correspondence to jjoo@korea.ac.kr

(1) Current-time ($I-t$) characteristic behaviors in simultaneous multi-surface anodization (SMSA)

As shown in Fig. 1c and S1, the current level in pre- and man-SMSA decreased gradually with increasing anodizing time, which is typical feature of SMSA. These results are closely related to the reduction of total anodizing area and stresses stored in multi-interfaces resulting in the suppression of ions migration.

● Relation between anodizing area and current in single SMSA

In order to calculate the total anodizing area in single SMSA procedure, we assumed as follows;

- i) Standard mild anodizing condition under sulfuric acid : 0.3 M, +25 V, and 0 °C
- ii) Anodizing time = 15 h / Thickness of each AAO = 80.0 μm
- iii) Not considering reduction of total anodizing area due to the pre-SMSA: Growth of pre-AAO is more sophisticated than main-SMSA, because non-textured surfaces result in the various situations of initial nanopores formation and their merging even under the same anodizing condition.

Table S1 Variation of dimensions and anodizing area due to the SMSA.

	on 5 surfaces		on 4 surfaces ^{a)}	
	Before SMSA	After SMSA	Before SMSA	After SMSA
Front (Back) [mm]	20.0 × 35.0	(20.0 – 0.16) × (35.0 – 0.08)	20.0 × 35.0 ^{b)}	(20.0 – 0.16) × (35.0 – 0.08)
Right/Left [mm]	1.0 × 35.0	(1.0 – 0.16) × (35.0 – 0.08)	1.0 × 35.0	(1.0 – 0.08) × (35.0 – 0.08)
Bottom [mm]	1.0 × 20.0	(1.0 – 0.16) × (20.0 – 0.16)	1.0 × 20.0	(1.0 – 0.08) × (20.0 – 0.16)
Total [mm ²]	1490.0	1461.0	790.0 ^{b)}	775.3
Reduction Ratio [%]	1.95		1.86	

^{a)} Back surface was coated with nail polish to protect against main-anodization.

^{b)} Total area was calculated excluding back surface.

As shown in Table S1, the reduction ratios of total anodizing area after main-SMSA on 4 and 5 surfaces were estimated to be 1.86% and 1.95%, respectively. Fig. 1c showed that the decrease of current level in main-SMSA on 4 and 5 surfaces were ~8% and ~15% in terms of anodizing time, indicating that the anodizing time also played important role.

The current in anodization results from electron transfer due to the oxidation at Al/Al₂O₃ and Al₂O₃/electrolyte interfaces as well as migration of ions (*e.g.*, Al³⁺, O²⁻, and OH⁻) through oxide and electrolyte.^{S1-S3} Stresses generated from volume expansion due to the anodic oxidation also influences on the ion transport in oxide layer.^{S3-S5} Therefore, stresses stored in multi-interfaces during SMSA on 5 surfaces were larger than those of 4 surfaces, which suppressed the migration of ions and current. This analysis is well agreed with stress-related current peak position depending on number of anodizing surfaces.

● **Relation between anodizing area and current in multiple SMSAs**

The current level at early stage of $n+1^{\text{th}}$ main-SMSA reflected the reduction of total anodizing area due to the n^{th} main-SMSA. As shown in Fig. S1b, current values of the 1st to the 6th main-SMSA at 200 s were 44.0, 42.2, 40.3, 37.4, 36.7, and 35.1 mA, respectively. The reduction ratios were calculated to be 4.1%, 4.5%, 7.2%, 1.9%, and 4.1%, which are reasonable considering both the reduction of anodizing area due to the two-step SMSA procedure and stress-related suppression of ions migration. Deviation of reduction ratio (for examples, 7.2% and 1.9%) seems to be originated from the variations of the anodizing temperature, and amount/concentration of the acidic electrolyte at each sequence.

References

S1 J. P. O'Sullivan and G. C. Wood, *Proc. R. Soc. London A*, 1970, **317**, 511-543.

S2 F. Li, L. Zhang and R. M. Metzger, *Chem. Mater.*, 1998, **10**, 2470-2480.

S3 W. Lee and S.-J. Park, *Chem. Rev.*, 2014, **114**, 7487-7556.

S4 J. E. Houser and K. R. Hebert, *Nature Mater.*, 2009, **8**, 415-420.

S5 K. R. Hebert, S. P. Albu, I. Paramasivam and P. Schmuki, *Nature Mater.*, 2012, **11**, 162-166.

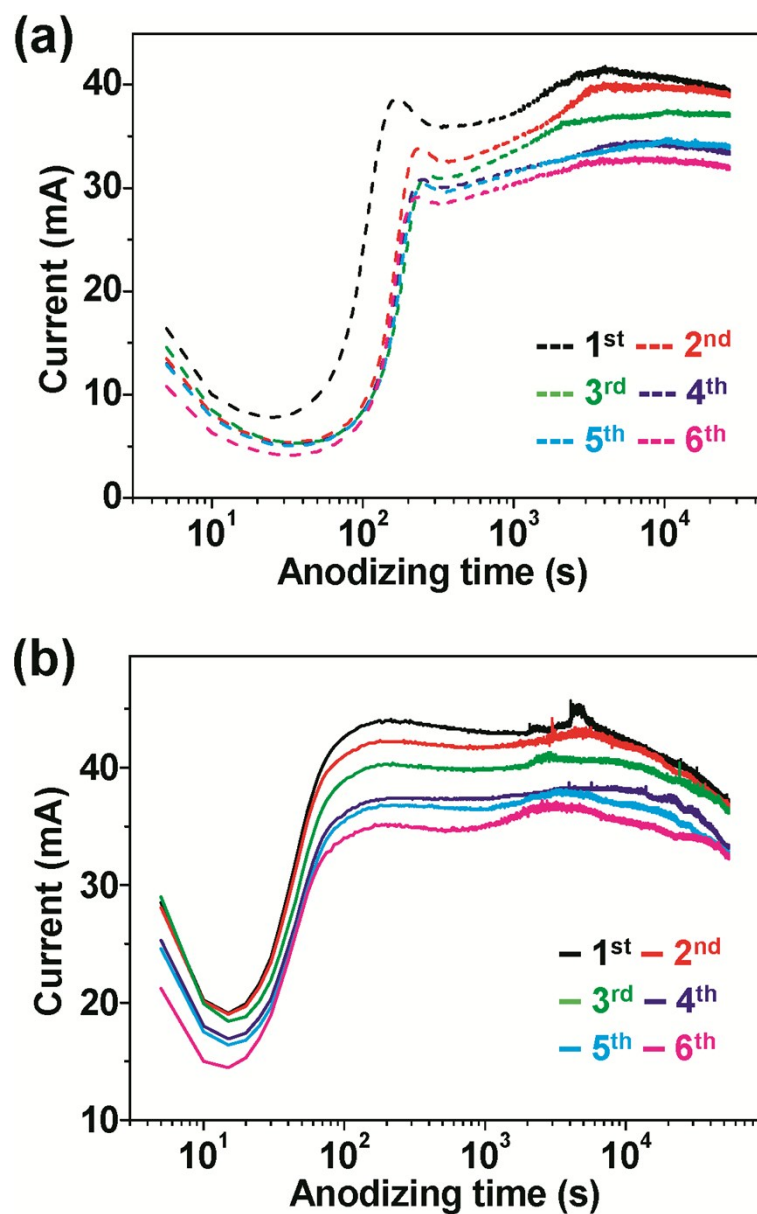


Fig. S1 Current–time ($I-t$) characteristics of pre- and main-SMSAs from the first to the sixth procedures. $I-t$ curves (logarithmic time-scale) of (a) pre-SMSAs and (b) main-SMSAs. As the SMSA procedure was repeated, the entire current level decreased owing to the reduction of the total anodizing area and stress-related suppression of ions migration.

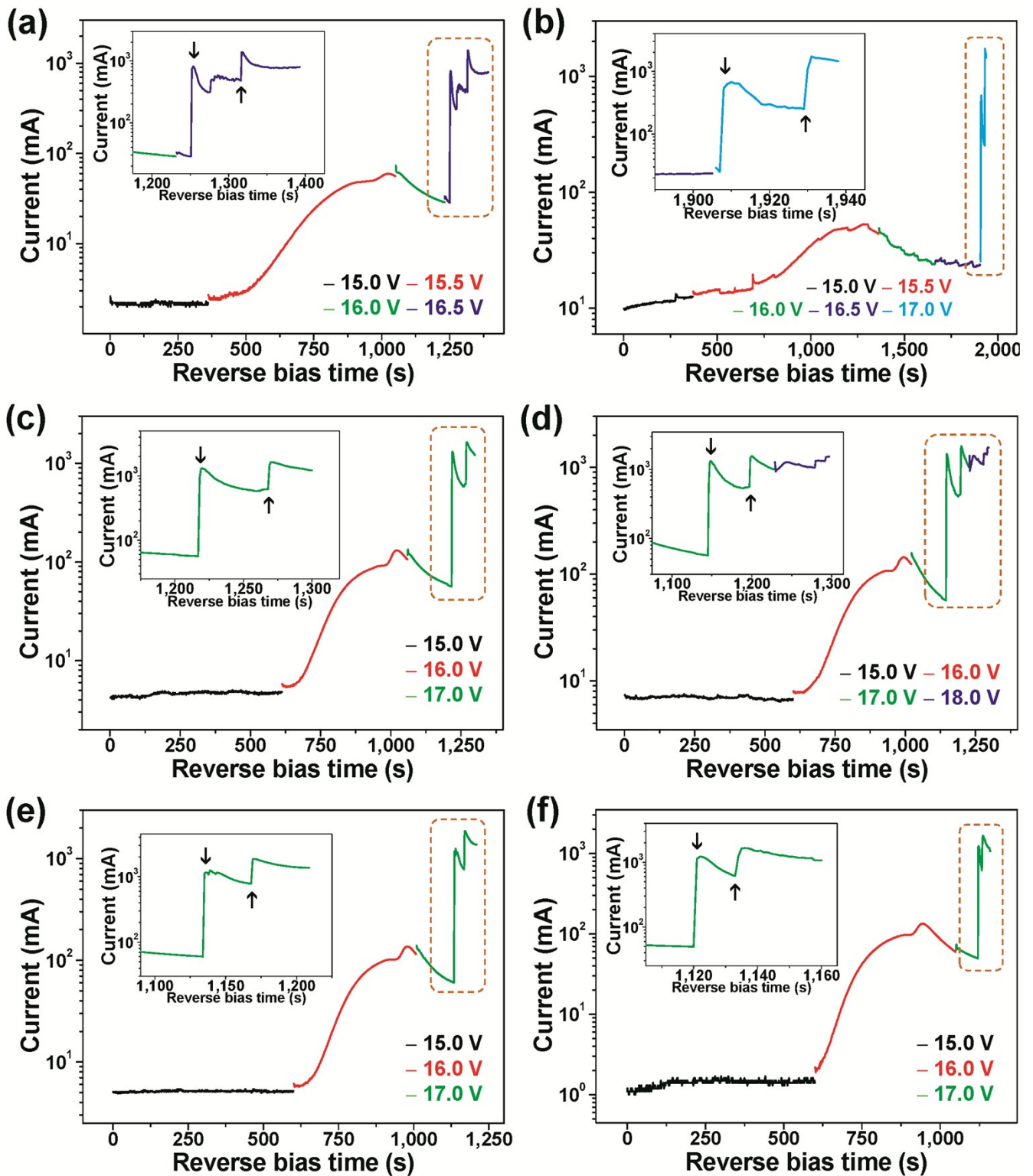


Fig. S2 $I-t$ characteristics during detachment of AAOs by applying SRBs. $I-t$ curves of the (a) first, (b) second, (c) third, (d) fourth, (e) fifth, and (f) sixth detachments. Insets: Magnified $I-t$ curves at the moments of detachment.

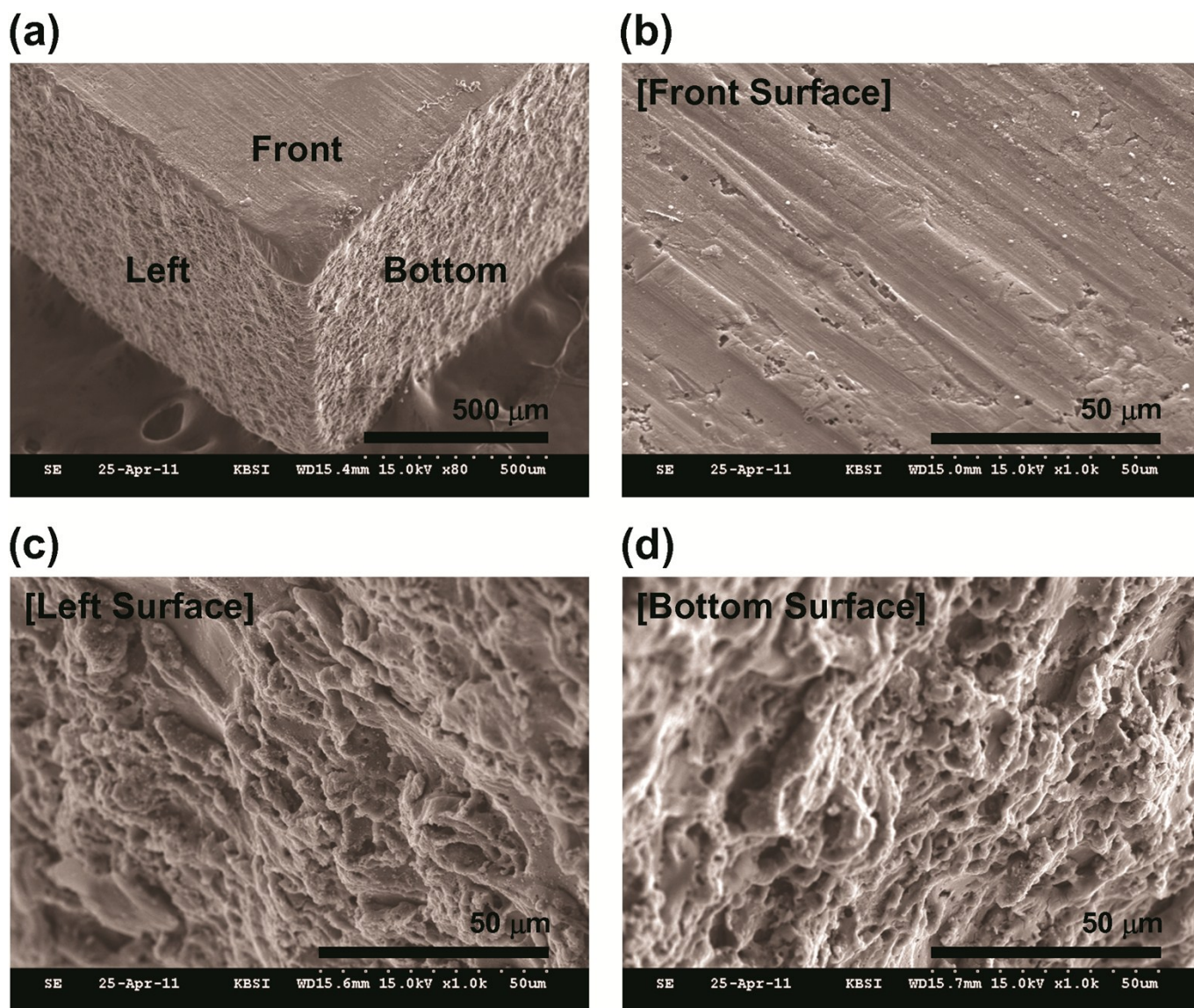


Fig. S3 Surface morphology of the pristine Al substrate. (a) A corner-view SEM image of the pristine Al substrate. Magnified SEM images of the (b) front, (c) left, and (d) bottom surfaces of the pristine Al substrate. The rough surfaces of the mechanically polished Al were observed.

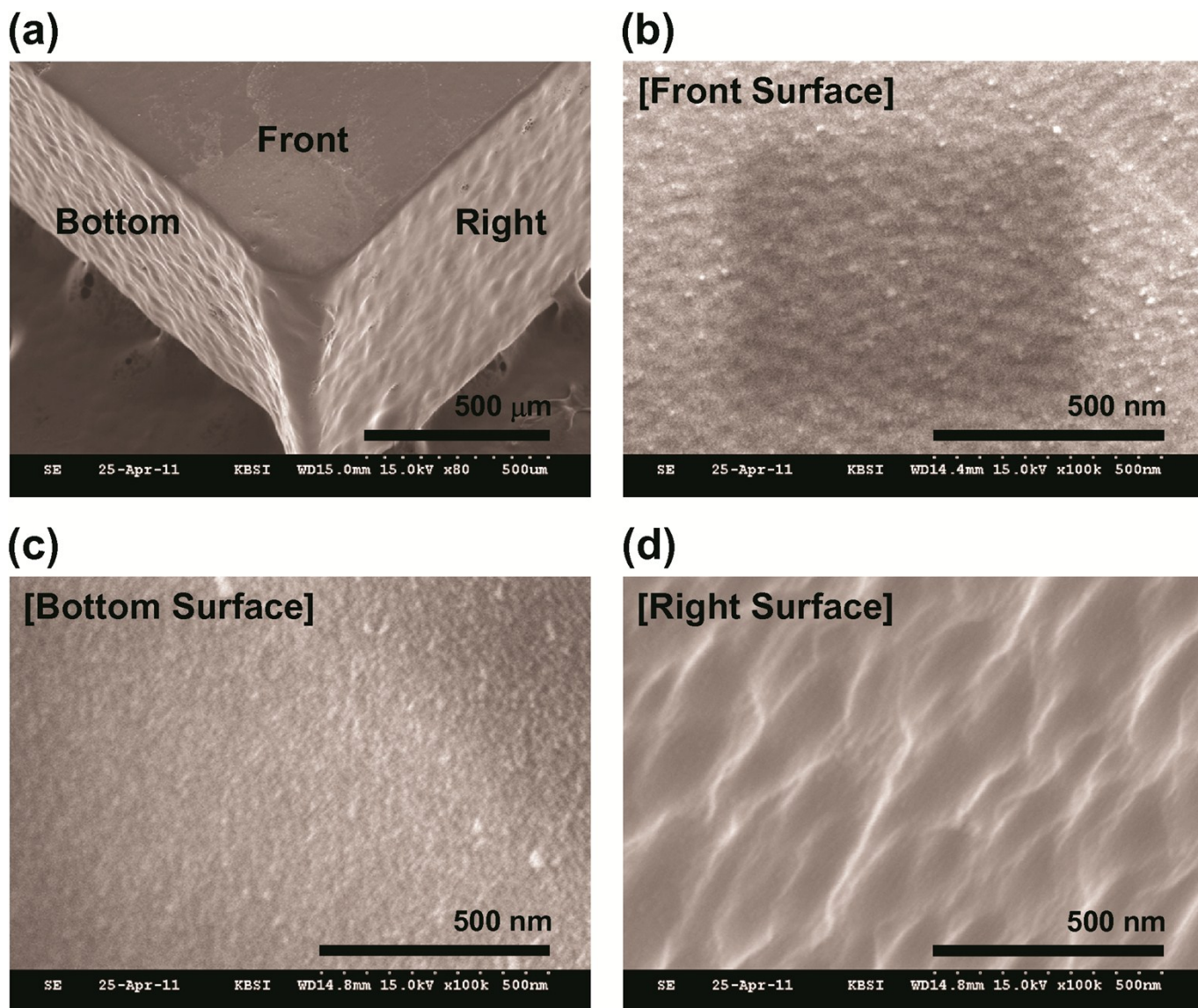


Fig. S4 Surface morphology of the electropolished Al substrate. (a) A corner-view SEM image of the electropolished Al substrate. Magnified SEM images of the (b) front, (c) bottom, and (d) right surfaces of the electropolished Al substrate. The roughness of each surface clearly decreased and very small concaves with irregular size and shape were observed.

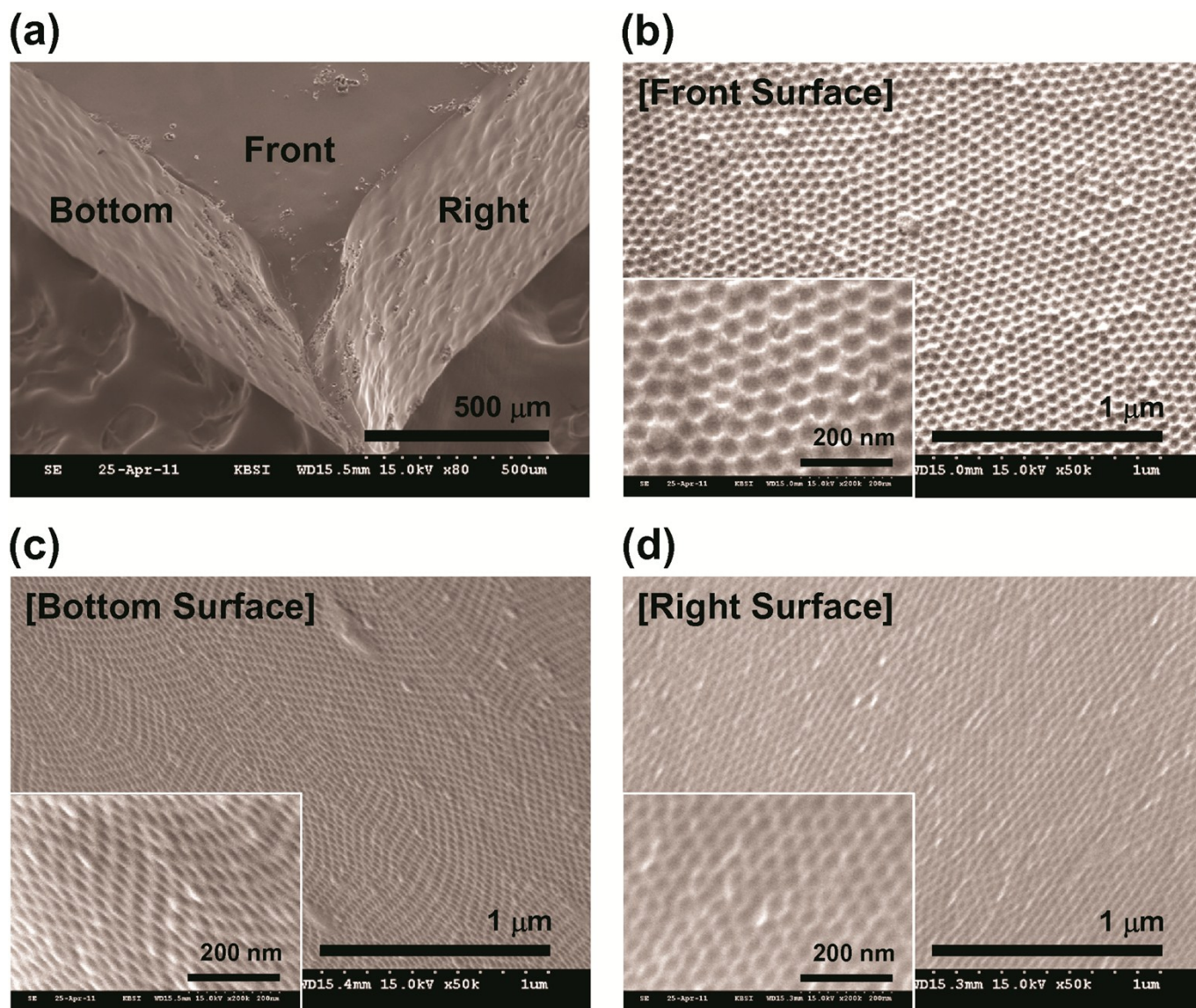


Fig. S5 Surface morphology of the textured Al substrate after the first pre-SMSA followed by chemical etching of pre-AAOs. (a) A corner-view SEM image of the textured Al substrate. Magnified SEM images of the (b) front, (c) bottom, and (d) right surface of the textured Al substrate. Insets: Magnified SEM images of the corresponding surfaces.

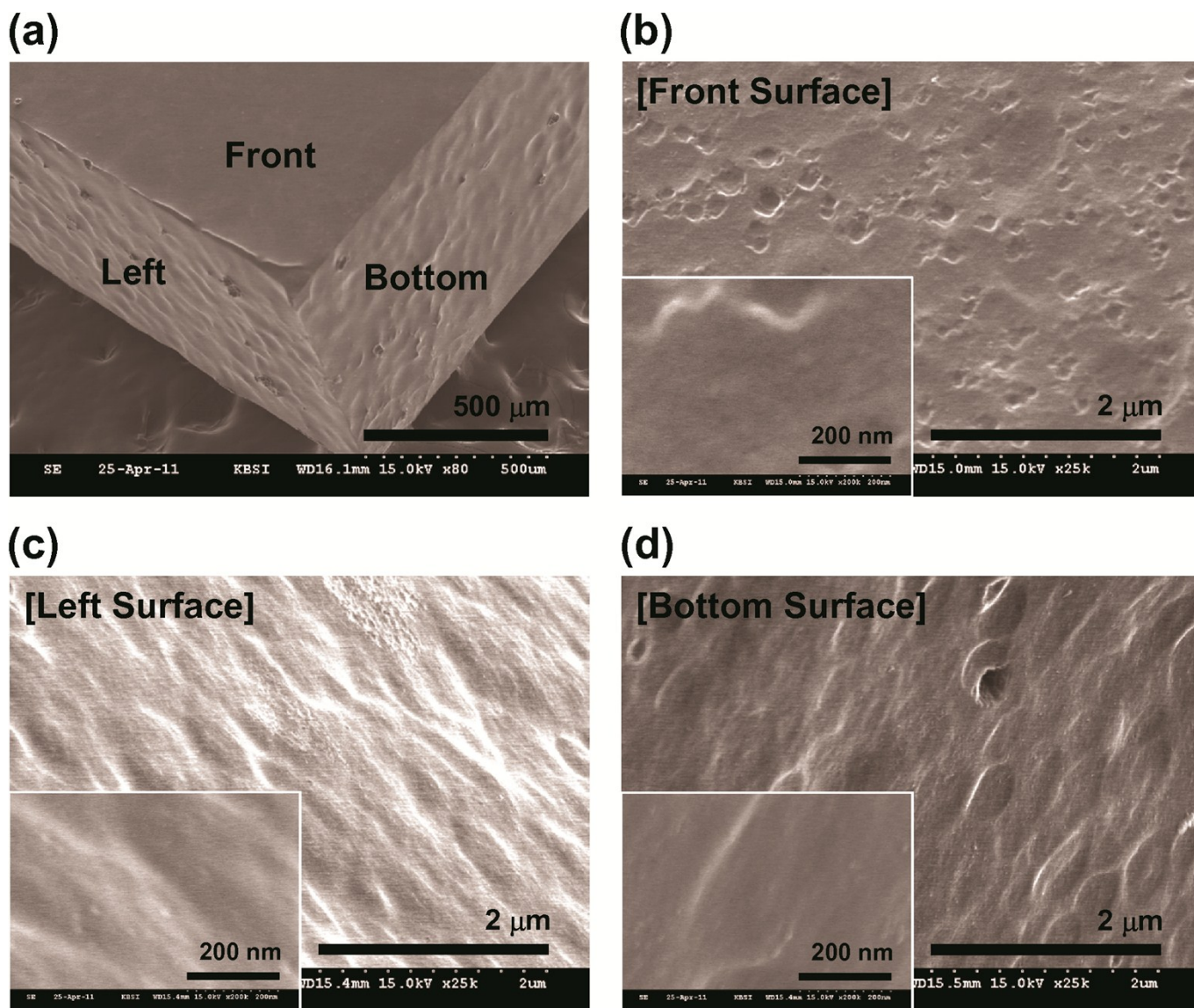


Fig. S6 Surface morphology of the Al substrate after the first main-SMSA followed by the detachment of main-AAOs and chemical etching of residual alumina. (a) A corner-view SEM image of the Al substrate. Magnified SEM images of the (b) front, (c) left, and (d) bottom surfaces of the Al substrate. Insets: Magnified SEM images of the corresponding surfaces of the Al substrate. The destruction of surface texturing was observed.

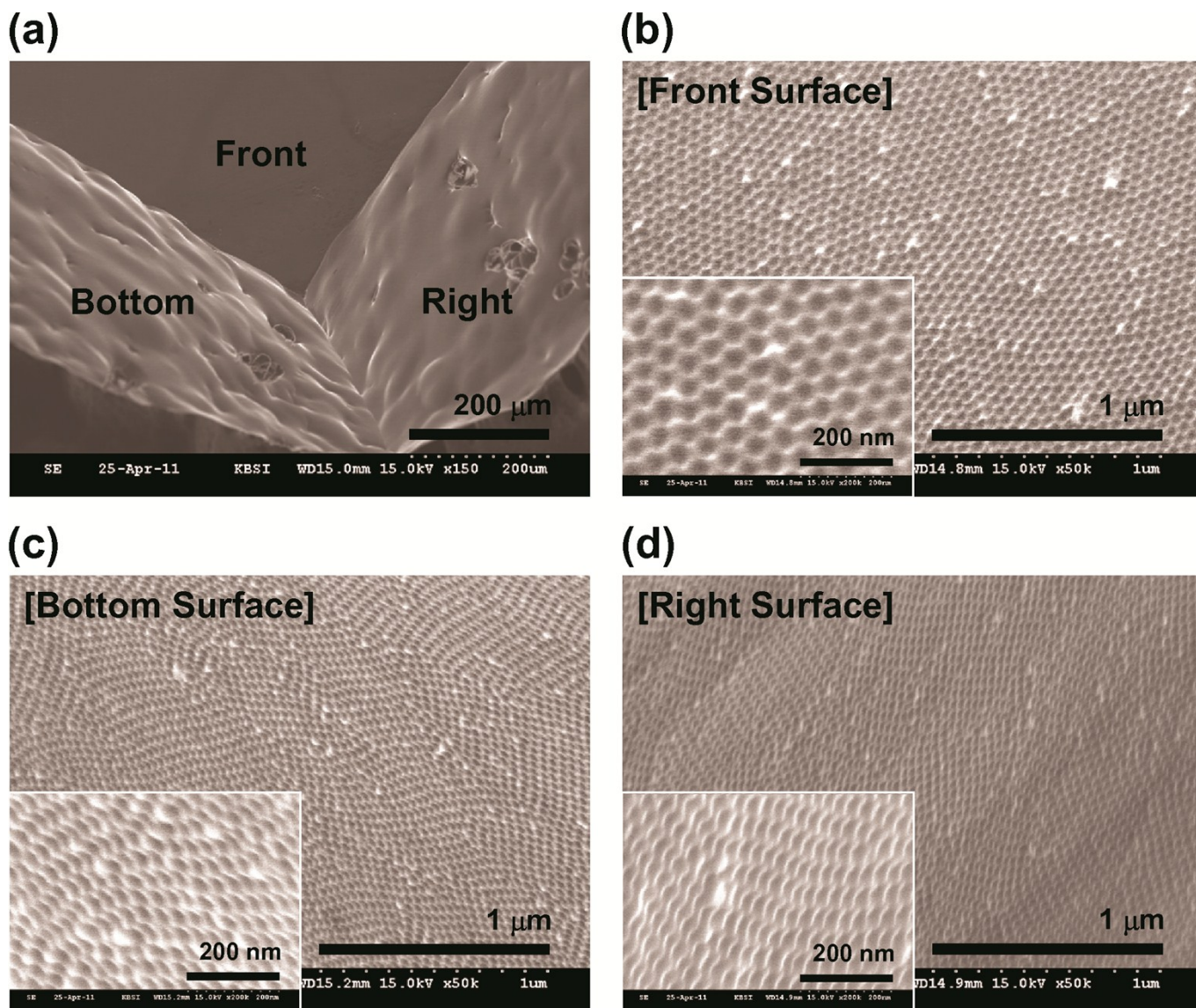


Fig. S7 Surface morphology of the re-textured Al substrate by the second pre-SMSA followed by chemical etching of pre-AAOs. (a) A corner-view SEM image of the Al substrate. Magnified SEM images of the (b) front, (c) bottom, and (d) right surfaces of the Al substrate. Insets: Magnified SEM images of the corresponding surfaces of the Al substrate.